

*Journal of*  
***Mechanics of***  
***Materials and Structures***

**POSTBUCKLING OF TRUSS-LATTICE SHEAR PANELS USING  
EXACT THEORY**

Philip A. Williams, Richard Butler, Hyunsun A. Kim and Giles W. Hunt

***Volume 3, N° 5***

***May 2008***



# POSTBUCKLING OF TRUSS-LATTICE SHEAR PANELS USING EXACT THEORY

PHILIP A. WILLIAMS, RICHARD BUTLER, HYUNSUN A. KIM AND GILES W. HUNT

A new solution is developed to model the stable postbuckling behaviour of a truss-lattice shear panel. The mode shapes are derived through load equilibrium conditions and are based on the load in the structural members. The load in each member of a single-cell panel can be calculated exactly, without the need for an iterative postbuckling path, and the method produces excellent results in initial and advanced postbuckling. Comparisons are drawn with an alternative analytical method and the commonplace finite element approach. A Rayleigh–Ritz method based on a Fourier approximation to the mode shape provides the useful progression from an unbuckled to a buckled structure giving excellent results in initial postbuckling, although is limited for advanced postbuckling. The standard finite element method for this problem produces accurate results but with limited detail around the buckling load owing to the presence of an imperfection in the shape of the initial mode, which is required to initiate the postbuckling analysis.

## 1. Introduction

Truss structures are widely recognised as being an efficient way to carry load, as they are lightweight and have high stiffness. A recent investigation has shown that a truss-lattice configuration exhibits a stable postbuckling behaviour under shear [Williams et al. 2007], similar to that of a continuous panel via development of a diagonal tension field [Wagner 1931; Kuhn et al. 1952]. It has been demonstrated that by arranging the members of a truss-lattice to align with the compression and tension diagonals of a shear panel, as shown in Figure 1, a similar diagonal tension field can be established [Kim et al. 2004]. With the tension members dominating, the postbuckling behaviour of the truss-lattice panel is stable.

A benefit of such a configuration is the potential weight savings. A preliminary study investigated a truss-lattice configuration with a set of diagonal members such as Figure 2 and compared it with a continuous shear panels for a range of loads [Williams et al. 2007]. It was shown that for a panel under relatively low shear load (with a shear flow less than 100 N/mm), a simple unbuckled truss-lattice can offer weight-saving of at least 59% over postbuckled continuous panels, increasing to 66% if postbuckling is permitted.

Analysis of geometrically nonlinear postbuckling of frame structures has been actively researched in the past few decades. A common subject of interest has been incremental-iterative techniques including stiffness-based finite element (FE) methods which can be used to model the postbuckling behaviour of the truss-lattice structures above. However, it is possible and useful, particularly for physical insight, to also describe the deformations and postbuckling behaviour analytically.

---

*Keywords:* postbuckling, truss lattice, shear panels, nonlinear analysis.

This research is sponsored by the IdMRC (Innovative Design & Manufacturing Research Centre) in the Department of Mechanical Engineering at the University of Bath, funded by the EPSRC (Engineering and Physical Sciences Research Council).

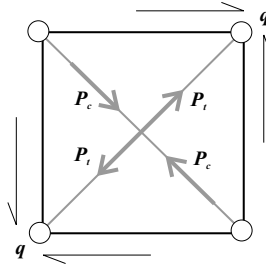


**Figure 1.** Shear flow  $q$  produces resultant axial forces  $P_c$  and  $P_t$  in a truss-lattice panel.

Developments in analyses of geometrically nonlinear frame structures, both in analytical understanding and in aspects of numerical techniques, have been summarised in an extensive review by Yang et al. [2003]. It is not therefore the intention to present a comprehensive survey of these developments here, but to introduce those methods that are relevant to this study.

The theory of beam columns is discussed in Timoshenko and Gere [1936] in which the elastic buckling behaviour and deflection of a beam under compressive loads can be described by sine and cosine functions of the applied load. This was extended by Williams [1964] to describe the nonlinear snap-through behaviour of a two-beam arch (or toggle). The beam theory stated in Timoshenko and Gere [1936] and used by Williams [1964] will be referred to as the exact solution, although there are some assumptions and approximations used in the formulation. Williams [1964], for example, follows the nonlinear behaviour of rigid jointed frameworks, which provides a good starting point for the struts to be considered here. The exact solution assumes a general mode shape described by trigonometric functions, which is defined in terms of the applied loads and boundary conditions of the members. No imperfection is required for the analysis, but the critical load of the structure must be found before analysing the postbuckling behaviour, and the assumption is made that deflections do not occur until the buckling load is reached. Only in-plane deflections are considered, and the examples given are such that the end-shortening and in-plane deflection of each member can be described exactly for a given applied load.

An alternative analytical procedure is the Rayleigh–Ritz analysis, which has been applied to many different postbuckling problems, including plates and struts [Thompson and Hunt 1973], although rarely with the introduction of a tension member. This analysis uses a Fourier expansion to approximate the mode shape, where the number of terms that are included determines the accuracy of the solution as the

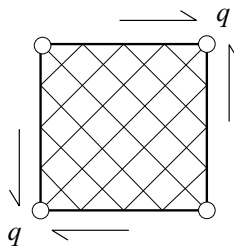


**Figure 2.** Multiple cell truss-lattice shear panel.

mode shape develops in postbuckling. By considering the total energy of the structure, it is possible to trace the in-plane prebuckling equilibrium solution, and hence measure the ratio of initial postbuckling to prebuckling stiffness.

The conventional approach to modelling this type of problem is via nonlinear FE analysis. The FE methodology is flexible and applicable to a wide range of problems, and a model can be set up in a relatively straight-forward manner with commercially available software. The analysis also gives an accurate result, although often at the expense of high computation time. To follow the postbuckling behaviour of a structure, one must first perform a buckling analysis to find the buckling load and mode shape. This mode shape can then be used as an imperfection, which is required for nonlinear postbuckling FE analysis. The requirement of an imperfection is one disadvantage with the FE approach as it causes out-of-plane bending deformation to occur before the critical load is reached. The FE method is mesh sensitive as it requires an appropriate number of correctly positioned elements; it can be costly, owing to the often high computation time; and the boundary conditions can often be difficult to model correctly, although it is not always apparent when mistakes are made.

This paper investigates the postbuckling behaviour of a truss-lattice shear panel by developing an analytical procedure using exact member theory. The mode shape of each member is dependent on the load in the member, and hence the postbuckling stiffness and deflection of each member can be calculated exactly for any given load. Comparisons are then drawn between the alternative analytical Rayleigh–Ritz method and FE analysis. Both analytical procedures are purpose driven and appropriate for modelling the truss-lattice in postbuckling and aimed at addressing some of the limiting features of the FE approach. Of particular interest is the use of fewer elements in the model definition, hence fewer equations to solve; the physical insight that each method introduces; and the principle of developing a method to be used specifically for the truss-lattice shear panel problem.

## 2. Truss-lattice shear panel

The truss-lattice considered in this paper comprises a series of diagonal struts arranged at  $\pm 45^\circ$  to the shear load, as shown in Figure 1, such that the resulting diagonal tension and compression are carried axially in the lattice members. We also consider a frame around the lattice consisting of rigid members with pinned corner joints. The shear flow  $q$  in Figure 1 is modelled as compression and tension loads  $P$ , which are applied at the corners and transferred to the internal members via the stiff frame as a displacement controlled mechanical system as shown in Figure 3. The lattice members are welded at their intersections but have a simply-supported connection to the frame. One crossover of diagonal members is referred to as one cell, highlighted in Figure 3(a), and the number of cells along one side of a square panel is given by the cell dimension  $n$ . The length of each member is  $\ell$ , and hence the frame members are length  $\sqrt{2}n\ell$ . Rotating the model by  $45^\circ$ , as shown in Figure 3(b), aligns the members with the global  $X$  and  $Y$  axis, and a shear deformation (given by effective shear strain  $\gamma$ ) produces displacements in these global directions ( $\Delta_X$  and  $\Delta_Y$  respectively). These displacements are considered positive in compression and hence  $\Delta_X$  is negative, as demonstrated in Figure 3(b).

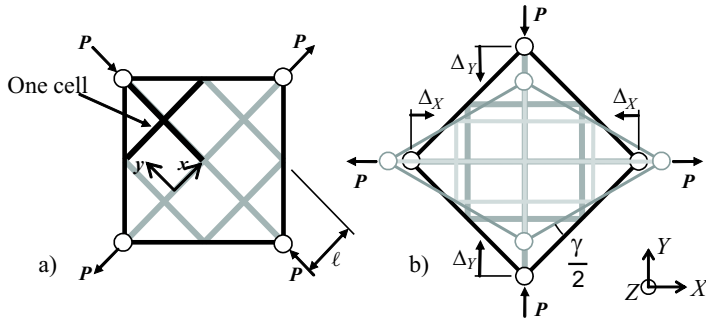


**Figure 3.** (a) Truss-lattice panel ( $n = 2$ ) with rigid frame members under external diagonal loads  $P$ ; (b) Deformed lattice, showing effective shear strain  $\gamma$ , and in-plane end displacements  $\Delta_x$  and  $\Delta_y$ .

### 3. Analytical methods

Analytical methods do not require imperfections and so have the ability to pin-point the initial buckling load and to trace the initial postbuckling path more accurately than FE methods. In addition, no frame is required for the analytical methods as the displacements are described by the geometric relationships associated with a rigid frame. The frame has a very high stiffness in the FE approach, but it is still finite, and so the properties of the frame do have some effect on the results. Removing the frame in the analytical methods removes this variable and allows some additional physical insight into the behaviour of the lattice itself, although one must consider the properties of the frame when a realistic panel is to be modelled.

**3.1. Exact initial mode method.** This approach initially solves the eigenvalue problem to produce an exact buckling load and critical mode shape based on a single element for each member. A development is then made to the existing method to extend the analysis into postbuckling through consideration of equilibrium, boundary conditions, and compatibility conditions. The same mode shape is assumed throughout, based on the initial buckling mode, although the amplitudes are dependent on the loads applied to the members, and the assumption is later verified by comparison with FE results. The analysis extends successfully into the nonlinear postbuckling regime, although we note that the large deflection nonlinearities associated with solutions of the elastica problem have been omitted [Thompson and Hunt 1973]. The analysis is thus suitable for moderately large postbuckling deflections.

**3.1.1. Equilibrium.** We consider a moment equilibrium about a cut  $C$  along a general lattice member (shown in Figure 4) such that

$$M = -EI \frac{d^2w}{dx^2} = Pw + m - P_z x, \tag{1}$$

where  $E$  is the elastic modulus and  $I$  is the second moment of area relating to out-of-plane deflections. The load in the member  $P$  is positive in compression  $P_c$  and negative in tension  $P_t$ . The out-of-plane force  $P_z$  (which is always positive in the  $z$ -direction) and the moment  $m$  act at the end of each member.

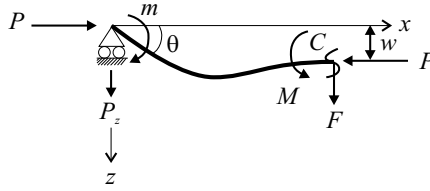


**Figure 4.** Forces and displacements for a general lattice member. The moment  $m$  at the pin joint is included for the general definition in Equation (1).

The whole structure must be in load equilibrium, hence the out-of-plane contributions  $P_z$  from each of the members must sum to zero. We shall return to this requirement later.

The following equations are applicable to both compression and tension members although the subscripts  $c$  and  $t$  respectively are used where appropriate. Equation (1) has a general solution

$$w = C_1 \cos \beta x + C_2 \sin \beta x - \frac{m}{P} + \frac{P_z x}{P} \tag{2}$$

in which

$$\beta^2 = P/EI, \tag{3}$$

and  $C_1$  and  $C_2$  are unknown coefficients to be found through application of the boundary conditions.

**3.1.2. Boundary conditions.** If we consider a single cell  $n = 1$  model (with local coordinate  $x$  as shown in Figure 3(a)) with pinned corners and symmetry around the central members, the boundary conditions for this case are as follows. The deflection  $w$  at  $x = 0$  is zero and solving for  $C_1$  gives

$$C_1 = m/P. \tag{4}$$

At  $x = l$  the gradient  $\dot{w}$  is zero owing to symmetry (where a dot represents differentiation with respect to  $x$ )

$$\dot{w} = -\frac{m\beta \sin \beta l}{P} + C_2 \beta \cos \beta l + \frac{P_z}{P} = 0,$$

and hence

$$C_2 = \frac{m\beta \sin \beta l - P_z}{P\beta \cos \beta l}. \tag{5}$$

Therefore, substituting Equations (4) and (5) into Equation (2) gives the following general equation for the out-of-plane deflection of a compression member

$$w_c = \frac{m_c}{P_c} \left( \cos \beta_c x + \frac{\sin \beta_c l \sin \beta_c x}{\cos \beta_c l} - 1 \right) + \frac{P_{zc}}{P_c} \left( x - \frac{\sin \beta_c x}{\beta_c \cos \beta_c l} \right). \tag{6}$$

As tension load  $P_t$  is considered negative in this analysis, the deflection of a tension member  $w_t$  is

$$w_t = \frac{m_t}{P_t} \left( \cos \beta_t x + \frac{\sin \beta_t l \sin \beta_t x}{\cos \beta_t l} - 1 \right) + \frac{P_{zt}}{P_t} \left( x - \frac{\sin \beta_t x}{\beta_t \cos \beta_t l} \right), \tag{7}$$

and  $\beta_t$  must be imaginary in accordance with Equation (3).

For a pin joint, the moment  $m$  is zero, which further simplifies Equations (6) and (7) to give

$$w_c = \frac{P_{zc}}{P_c} \left( x - \frac{\sin \beta_c x}{\beta_c \cos \beta_c \ell} \right), \quad w_t = \frac{P_{zt}}{P_t} \left( x - \frac{\sin \beta_t x}{\beta_t \cos \beta_t \ell} \right). \tag{8}$$

**3.1.3. Compatibility.** A compatibility condition is applied at the intersection of the lattice members where the central out-of-plane deflection  $w^*$  must be the same for both members and is defined by Equations (6) and (7) at  $x = \ell$ . Differentiating Equations (6) and (7) at  $x = 0$  gives the angle of rotation  $\theta$ , and applying the compatibility condition and rearranging gives

$$m = \frac{(\sin \beta \ell - \beta \ell \cos \beta \ell)}{P \beta Z} \theta - \frac{(1 - \cos \beta \ell)}{P Z} w^* \tag{9}$$

and

$$P_z = \frac{(1 - \cos \beta \ell)}{P Z} \theta - \frac{\beta \sin \beta \ell}{P Z} w^*, \tag{10}$$

where  $Z$  is the determinant of the basic member matrix with the solution

$$Z = \frac{(2 - 2 \cos \beta \ell - \beta \ell \sin \beta \ell)}{P^2}. \tag{11}$$

**3.1.4. Initial buckling.** From the Wittrick–Williams algorithm for calculating the critical buckling load of elastic structures [Wittrick and Williams 1973], the critical load of the truss-lattice can be determined by first constructing a stiffness matrix for the whole structure and then finding the values for load that give zero values for the determinant of this matrix. This procedure finds the critical loads and produces corresponding mode shapes for the structure. It does not determine the amplitudes of the modes nor any postbuckling behaviour.

**3.1.5. Postbuckling.** Applying the boundary condition for a pin joint,  $m = 0$ , to Equation (9) gives

$$\theta = \frac{\beta(1 - \cos \beta \ell)}{(\sin \beta \ell - \beta \ell \cos \beta \ell)} w^*. \tag{12}$$

Substituting Equation (12) into Equation (10) gives  $P_z$  in terms of  $w^*$  and the applied load  $P$  such that

$$P_z = \left( \frac{(1 - \cos \beta \ell)^2}{(\sin \beta \ell - \beta \ell \cos \beta \ell)} - \sin \beta \ell \right) \frac{\beta w^*}{P Z}. \tag{13}$$

We now consider the out-of-plane equilibrium. Owing to symmetry, the out-of-plane reactions  $P_{zc}$  produced when the compression members buckle must be equal for the two compression ends in the single cell model, as must the reactions for the tension members  $P_{zt}$ . Hence for equilibrium,

$$P_{zc} = -P_{zt}. \tag{14}$$

Therefore the values of load in the members must produce  $P_z$  in Equation (13) such that Equation (14) is satisfied, and hence there is a transcendental relationship between  $P_t$  and  $P_c$ .

In Figure 3(b), the displacements in the  $X$  and  $Y$  directions are geometrically linked due to the rigid frame member. Describing these in terms of the effective shear strain  $\gamma$  gives

$$\Delta_Y = \ell \left[ 1 - \sqrt{2} \sin \left( \frac{\pi}{4} - \frac{\gamma}{2} \right) \right] \approx \ell \left( \frac{\gamma}{2} + \frac{\gamma^2}{8} \right), \quad \Delta_X = \ell \left[ 1 - \sqrt{2} \cos \left( \frac{\pi}{4} - \frac{\gamma}{2} \right) \right] \approx -\ell \left( \frac{\gamma}{2} - \frac{\gamma^2}{8} \right), \tag{15}$$

where the first three terms of the power series expansion are used for the trigonometric factors. We note that a positive (compression) load produces a positive displacement in  $Y$ , and conversely a negative (tensile) load produces a negative displacement in  $X$ .

The displacements of the ends of the members can also be described as the sum of the end-shortening required to form the deflected mode shape and the axial strain due to the load in the member

$$\Delta_Y = \frac{1}{2} \int_0^\ell \dot{w}_c^2 dx + \frac{P_c \ell}{EA}, \quad \Delta_X = \frac{1}{2} \int_0^\ell \dot{w}_t^2 dx + \frac{P_t \ell}{EA}, \tag{16}$$

where  $A$  is the cross-sectional area of the truss members.

The transcendental nature of Equations (1)–(16) makes a direct solution impossible. Instead, an iterative procedure is adopted such as that detailed in Figure 5. The mode shapes must first be defined in terms of the loads  $P_c$  and  $P_t$  and the central deflection  $w^*$  (substituting Equations (11) and (13) into Equations (8)). Problem-specific values must then be assigned to the variables  $EI$ ,  $EA$ ,  $\ell$ , and the critical load calculated. An initial value for  $P_t$  must first be assumed (just above the critical load  $P^{crit}$ ), and  $P_{zt}$  is calculated using Equation (13). The corresponding  $P_c$  is computed iteratively to determine  $P_{zc}$  such that

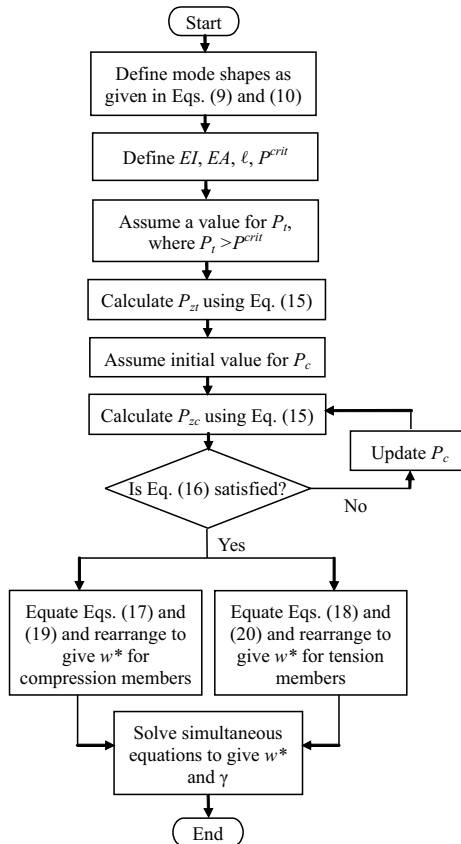


**Figure 5.** Flow diagram for the iterative procedure required to solve the postbuckling exact initial mode method.

the equilibrium condition in Equation (14) is satisfied. The analysis can be extended by incrementally increasing values for  $P_t$  as the load in tension is expected to increase, but the analysis is not dependent on the size of the step.

Once the values of the loads are known, the deflections and displacements are found by first equating the corresponding  $\Delta_X$  and  $\Delta_Y$  displacements in Equations (15)–(16) and rearranging to give  $w^*$  in terms of  $\gamma$ , then solving the two subsequent simultaneous equations. With incremental values for  $P_t$ , the postbuckling performance is traced until a limiting criterion is reached. The applied load  $P$  is taken as the mean of the tension and compression loads and is used as an indication to the extent of progress into the postbuckling region with five times the critical load defined as the end condition for the iterative procedure of Figure 5. The process requires significant algebraic manipulation and a numerical solution which has been implemented within the algebraic manipulation package Maple [Maple 2005].

**3.2. Rayleigh–Ritz method.** This approach uses a Fourier expansion approximation to the mode shape and considers a minimum energy solution to the development of the mode in postbuckling. With the modal development described by its shape alone rather than including the load in the members as in the previous analyses, the Rayleigh–Ritz method provides a useful visual tool and provides information which is overlooked by the other methods.

The mode shape of the tension and compression members in Equations (8) can be expressed in a more simplified form by the  $N$  degree-of-freedom Fourier approximation,

$$w_c = Q_1 \ell \sin\left(\frac{\pi x}{2\ell}\right) + Q_3 \ell \sin\left(\frac{3\pi x}{2\ell}\right) + Q_5 \ell \sin\left(\frac{5\pi x}{2\ell}\right) + \dots + \left(\sum_{i=1}^N Q_i\right) \ell \sin\left(\frac{(N+1)\pi x}{2\ell}\right) \quad (17)$$

$$w_t = Q_2 \ell \sin\left(\frac{\pi x}{2\ell}\right) + Q_4 \ell \sin\left(\frac{3\pi x}{2\ell}\right) + Q_6 \ell \sin\left(\frac{5\pi x}{2\ell}\right) + \dots \quad (18)$$

with ( $i = 1 \dots N$ ,  $N$  even) where the  $Q_i$  are the amplitudes of the modal contributions [Thompson and Hunt 1973], written in terms of the total strut length ( $2\ell$ ). Equal central deflection in the two components is enforced by the final term in the  $x$ -series, where negative values for the even-numbered  $Q_i$  would be expected in the final solution.

If we consider the potential energy  $V$  of the deformed shape for the whole model, there is bending energy  $U_B$  and axial (or membrane) energy  $U_M$  with work done by the applied load  $P\varepsilon = P\Delta_X + P\Delta_Y$ , such that  $V = 2U_B + 2U_M - 2P\varepsilon$ , where

$$U_B = \frac{EI}{2} \int_0^\ell \dot{w}_c^2 dx + \frac{EI}{2} \int_0^\ell \dot{w}_t^2 dx, \quad U_M = \frac{EA}{2\ell} \left(\Delta_X - \frac{1}{2} \int_0^\ell \dot{w}_c^2 dx\right)^2 + \frac{EA}{2\ell} \left(\Delta_Y - \frac{1}{2} \int_0^\ell \dot{w}_t^2 dx\right)^2.$$

It should be noted that in-plane stretching is automatically included dependent on the axial stiffness  $EA$  and monitored by a single extra degree of freedom that averages the corner shearing displacements,  $\Delta = (\Delta_Y - \Delta_X)/2$ .

By introducing a set of sliding incremental coordinates a linear approximation to the nontrivial fundamental (prebuckling) solution is then readily accommodated [Thompson and Hunt 1973]. Unlike the previous analysis which assumed zero deflection before buckling, this allows important comparisons between pre- and postbuckling stiffness.

The unbuckled (fundamental) equilibrium path is found by minimising the energy with respect to  $\Delta$  with the out-of-plane displacements set to zero. Postbuckling equilibrium states are then represented by the set of  $N$  nonlinear equations that come from setting the derivatives of  $V$  with respect to  $Q_i$  equal to zero. Rather than attempting to find an exact or numerical solution, an ordered Taylor series approximation to the postbuckling equilibrium path is obtained from these by applying the so-called perturbation technique, based on expansion of the energy function about the critical equilibrium state [Thompson and Hunt 1973]. All analysis is carried out within the algebraic manipulation package Maple [Maple 2005].

#### 4. Finite element method

The truss-lattice has been modelled with the FE software ABAQUS using simple Euler–Bernoulli beams [ABAQUS 2003] with eight elements for each length  $\ell$  giving sufficiently accurate results for the buckling analysis. The frame members are pinned at the corners to allow displacements in the  $XY$  plane. These members are modelled with high axial and bending stiffness to simulate a rigid loading frame. Constraints are applied to the model at the four corners to prevent displacements in  $X$  and  $Z$  at the top and bottom and in  $Y$  and  $Z$  at the sides, and symmetry is enforced about the central members. Only buckling out of the  $XY$  plane is considered (although buckling in-plane is also possible, as demonstrated in Williams et al. [2007]) by specifying the second moment of area of the lattice members  $I$  to be much greater in-plane than out-of-plane. A linear eigen-buckling method is used to find the critical buckling loads and corresponding mode shapes, and the initial mode shape is imported as an imperfection for the nonlinear Riks method for postbuckling analysis [Riks 1979].

#### 5. Results and discussion

The FE results from ABAQUS are compared with those from the Maple solutions of the exact method and the energy method for one cell.

**5.1. Mode shapes.** The mode shapes in Figure 6(a) demonstrate that when the compression members buckle out-of-plane, the mode is initially global (long wavelength) then moving into a more localised short-wave mode in postbuckling, Figure 6(b). This development from global to local mode is particularly prominent with increasing numbers of cells such as the  $n = 3$  and  $n = 4$  models in Figure 6, where some elements change from positive deflection to negative as the localised mode develops.

**5.2. Analytical method results.** In a single cell the initial buckling mode from both methods is a global buckle in which the compression member is dominated by a half sine mode with a slight dip in the centre due to the presence of higher modal contributions (as given in Equation (17)). As the postbuckling develops the central node is constrained by the tension member so that the shape becomes more localised with large deflections developing in the mid-regions of the compression member but a reducing deflection at the central node. This is modelled in the Rayleigh–Ritz method through the development of the higher modal contributions and is driven by the additional load carried in the tension member. All three formulations performed satisfactorily in describing the mode shapes and their development in postbuckling from global to local.

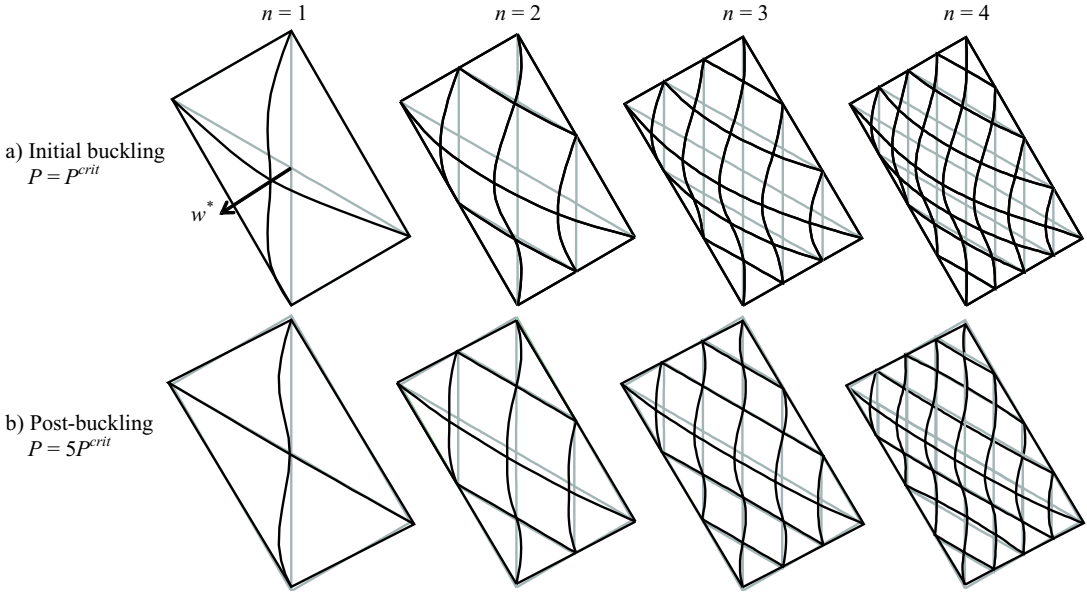


**Figure 6.** Initial buckling and postbuckling mode shapes with increasing numbers of cells. The central out-of-plane deflection  $w^*$  is shown for the initial mode of the  $n = 1$  lattice. The initial buckling and postbuckling modes are not shown to the same scale.

In calculating the critical load using the exact initial mode and FE methods, it has been assumed that there are no geometric displacements prior to buckling. However, in practice the in-plane stiffness of the members will determine the displacements that occur. This prebuckling deformation is considered here using the Rayleigh–Ritz analysis. Table 1 gives both the critical load and the pre- to postbuckling ratio from the Rayleigh–Ritz analysis as the in-plane ( $EA$ ) stiffness is altered in comparison to the bending stiffness ( $EI$ ) of the lattice members. The critical load is nondimensionalised with respect to the Euler load for the total length  $2\ell$ .

With a lower in-plane stiffness, larger axial deformations are permitted prior to buckling. The members are linearly elastic, and with the geometric conditions defined in Equations (15) a greater proportion of the applied load is stored in the compression rather than tension members. With additional load in compression, buckling occurs at a lower value of applied load when the in-plane stiffness is lower, hence the reduced critical loads in Table 1.

Ratio $A\ell^2/I$	Critical load/Euler load	Post/prebuckling stiffness ratio
$10^5$	6.246	0.834
$10^4$	6.207	0.833
$10^3$	5.846	0.827

**Table 1.** Critical load and ratio of pre- to postbuckling stiffness for the Rayleigh–Ritz method.

Number of elements	Percentage error in buckling load
2	1.474
3	0.356
4	0.120
5	0.050
6	0.024
7	0.014
8	0.008
9	0.005
10	0.003

**Table 2.** Error in buckling load with increased number of elements.

The Rayleigh–Ritz method has the advantage of providing a natural comparison of postbuckling to prebuckling stiffness. For the one cell model, this is approximately 0.83, as shown in Table 1. As we move further into postbuckling and the tension member carries most of the additional load, the ratio would be expected to approach a value of 0.5.

**5.3. Finite element results.** Two factors influence the performance of the FE analysis of the problem: The number of elements used to construct the model, and the imperfection required for postbuckling analysis.

Beam elements with a cubic polynomial shape function are used to model the lattice members in FE. Sufficient elements must be used to achieve the correct mode shape, and the more localised the buckling becomes, the more elements are required. Eight elements per length  $\ell$  are sufficient to be within 0.01% of the buckling load calculated using the exact initial mode solution, as shown in Table 2.

Williams et al. [2007] identified that the first symmetric mode of the eigen-analysis is sufficient to initiate the out-of-plane postbuckling analysis which is the subject of interest in this study and is thus used here. The effect of different levels of imperfection in postbuckling is presented in Figure 7 with amplitude ranging from 0.01% to 0.3% of the length  $\ell$ . Higher values of imperfection cause greater rounding of the curve at the bifurcation point and a slight overshoot of the maximum deflection, so there is a definite loss of accuracy associated with the use of an imperfection as shown in Figure 7. It is not obvious what level of imperfection is required when constructing a particular model: With too small an imperfection the Riks method in ABAQUS fails to converge, and with too great an imperfection there is a loss of accuracy around the critical load. For the single cell analysis an imperfection with amplitude of approximately 0.01% of the length  $\ell$  was found to be the minimum that could be used for the analysis.

**5.4. Discussion.** Under shear load, the truss-lattice panel exhibits a global initial buckling mode as seen in the  $n = 1$  model in Figure 6(a). All three methods demonstrate a half sine dominated mode shape in the compression member with a partial constraint imposed by the tension member. The global mode is further demonstrated for models with more cells using the FE method in Figure 6(a).

Increasing the load beyond the critical load takes the lattice into the postbuckling regime and a more localised short-wave mode shape is adopted. The  $n = 3$  and 4 models in Figure 6, for example, progress

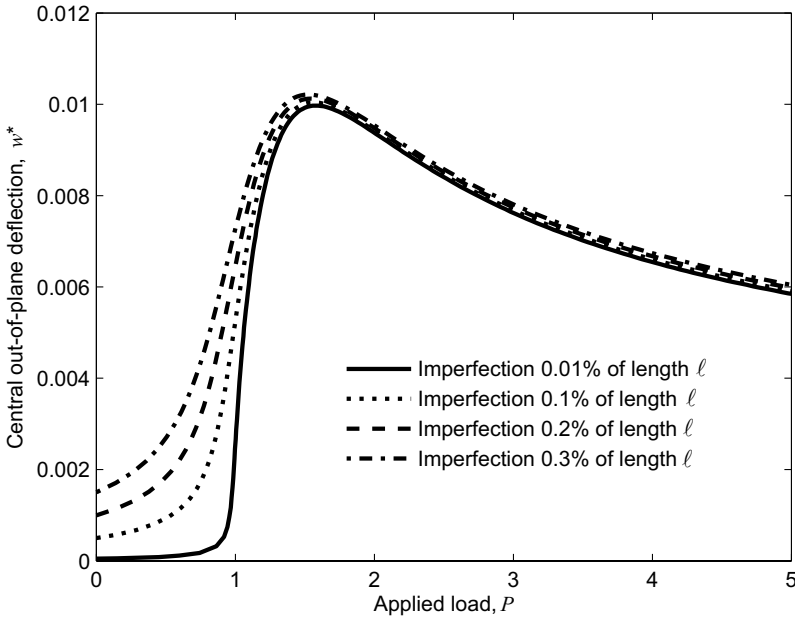


**Figure 7.** The effect of imperfection on the postbuckling behaviour in an FE analysis. Applied load is nondimensionalised with respect to the critical load, and deflection with respect to the total member length  $2\ell$ .

from just one antinode along the central compression member at initial buckling to five antinodes in postbuckling. For the single cell models in Figure 6 the localisation is due to the restriction imposed by the dominating tensile member which acts to reduce the central deflection.

When the compression member buckles, little additional load can be carried in the member. This is demonstrated in Figure 8 which shows the load carried in the compression and tension members against the average applied load. These are all nondimensionalised with respect to the critical load. For both the FE and exact method results the load in the buckled compression member is shown to remain approximately constant which results in transfer of load from the compression member to the tension member. The tension member thus gives the whole structure both stiffness and stability in postbuckling similar to the diagonal tension field developed in a continuous shear panel [Kuhn et al. 1952].

The central out-of-plane displacement of the single cell model for each of the three methods is plotted against the average applied load (nondimensionalised against the critical load) in Figure 9, for values of  $A\ell^2/I$  of the order of  $10^4$  (see Table 1). Whilst the critical load eigenvalue solutions from the FE and exact methods are apparently not affected by the axial stiffness of the members, Table 1 demonstrates that in reality they would be, with reduced buckling load with lower in-plane stiffness. For each of the three methods the increasing tensile load acts first to constrain and then to suppress the out-of-plane deflection of the central node  $w^*$  as a localised buckle develops.

The exact initial mode method requires no imperfection and so adopts the correct postbuckling path from outset. The governing equations (Equations (1)–(16)) require a deflection of the central node in order to calculate the loads and mode shapes but this is assumed to be zero until the buckling load is

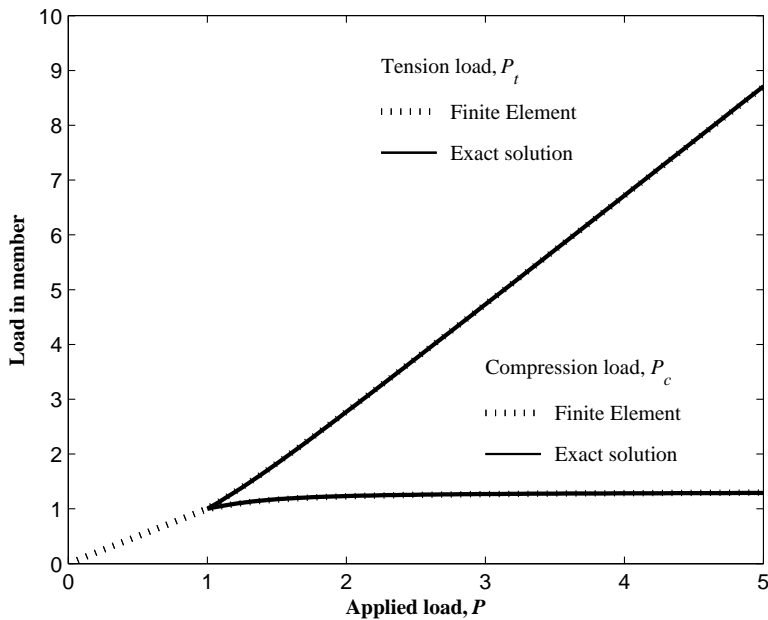


**Figure 8.** Load in compression and tension members after buckling. All loads nondimensionalised with respect to critical load.

reached. These equations are therefore limited to the postbuckling region and linear elastic theory must be used instead to find the load distribution and displacements before buckling. An initial buckling analysis must first be performed to determine the critical load, and hence two stages are required in the calculation of the postbuckling path.

The Rayleigh–Ritz method also requires no imperfection, and can follow both the prebuckling and initial postbuckling performance. The results presented in Figure 9 are first-order perturbation approximations, which are sufficient for the initial postbuckling results [Thompson and Hunt 1973]. The initial postbuckling stiffness is correct [Thompson and Hunt 1973], with a buckling mode developing at the critical load. However, whereas the two other methods compare well over the complete postbuckling range, this first-order Rayleigh–Ritz method is only approximate as the buckling develops and the subsequent deflection is always higher than the other results. Whilst the energy approach can be used to model large curvatures [Thompson and Hunt 1973], the development of the mode shape from global to local and the associated reduction in  $w^*$  are difficult to model with a Fourier approximation over the whole postbuckling range.

The FE method does require an imperfection as discussed earlier, and the level of imperfection has a dramatic effect on the prebuckling and initial postbuckling performance. Ultimately the presence of an imperfection, even if small, affects the accuracy of the results. (The imperfection used in Figure 9 was the minimum, at 0.01% of the length  $\ell$ .) However, with small imperfection the FE results converge quickly upon the other results soon after buckling, and the accuracy appears to be maintained well into postbuckling.

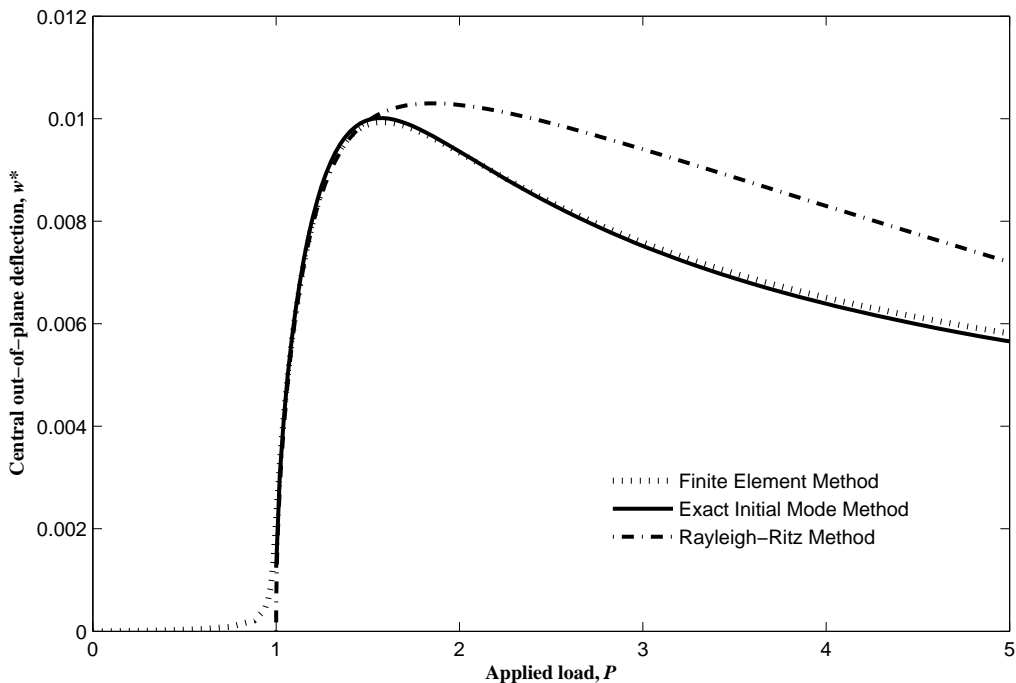


**Figure 9.** Out-of-plane deflection against applied load at the critical value. Loads nondimensionalised with respect to critical load and deflection with respect to total member length  $2\ell$ .

## 6. Conclusions

The stable postbuckling behaviour of truss-lattice shear panels has been studied using three complementary analysis techniques each contributing something different to the understanding of the behaviour of the lattice in postbuckling.

The truss-lattice shear panel has been developed and tested within an FE context and has similar buckling and postbuckling characteristics to a continuous shear panel. The FE postbuckling analysis must be considered in two parts owing to an initial imperfection being required for the nonlinear analysis. The presence of the imperfection then serves to reduce accuracy in the vicinity of the critical buckling load.

The initial buckling load and mode shape for a single cell model can be extracted exactly using the Wittrick–Williams algorithm, and the newly developed theory gives excellent correlation with the FE results in the postbuckling range. Again, two stages are required in the analysis, but the absence of imperfection allows the postbuckling response to be followed accurately. The tension member dominates in postbuckling, and the subsequent reduction in amplitude of the centre of the lattice permits the use of the equations without the need to consider large curvature.

The Rayleigh–Ritz energy method also accurately predicts the critical buckling load and initial postbuckling path and enables an evaluation of the ratio of pre- to postbuckled stiffness. The Fourier approximation enables a useful analysis based on the shape into which the mode develops. However, the

advanced postbuckled mode shape is not suited to the Fourier approximation used, and the increase in the number of terms required would make this method much less efficient than the others in determining the behaviour of the truss-lattice far into the postbuckling range.

The results demonstrate the usefulness of considering complementary methods when conducting non-linear analyses. The standard FE approach is relatively straightforward to establish and with sufficient elements produces accurate postbuckling results. The accuracy of the FE method is limited only by the required imperfection which does not form part of the exact solution or Rayleigh–Ritz analyses. The exact solution method shows excellent correlation in postbuckling, and the Rayleigh–Ritz method provides the link between pre- and postbuckling with accurate predictions for the initial postbuckling behaviour.

## References

- [ABAQUS 2003] ABAQUS, *Version 6.4 Documentation*, ABAQUS Inc., 2003.
- [Kim et al. 2004] H. A. Kim, R. Butler, and P. A. Williams, “Buckling and post-buckling analysis of shear panels for optimisation”, in *Computational mechanics, WCCM VI in conjunction with APCOM'04*, Beijing, China, 2004.
- [Kuhn et al. 1952] P. Kuhn, J. P. Peterson, and L. R. Levin, “A summary of diagonal tension: Part 1 - methods of analysis”, Technical report NACA TN-2661, 1952.
- [Maple 2005] Maple, *Maplesoft Version 10 Documentation*, Maple, 2005. Division of Waterloo Maple Inc.
- [Riks 1979] E. Riks, “An incremental approach to the solution of snapping and buckling problems”, *Int. J. Solids Struct.* **15**:7 (1979), 529–551.
- [Thompson and Hunt 1973] J. M. T. Thompson and G. W. Hunt, *A general theory of elastic stability*, Wiley, London, 1973.
- [Timoshenko and Gere 1936] S. P. Timoshenko and J. M. Gere, *Theory of elastic stability*, McGraw-Hill Book Company, Inc., NY, 1936.
- [Wagner 1931] H. Wagner, “Flat sheet metal girders with very thin web: Part III - sheet metal girders with spars resistant to bending. The stress in uprights - diagonal tension fields”, Technical report NACA TM-606, 1931.
- [Williams 1964] F. W. Williams, “An approach to the non-linear behaviour of the members of a rigid jointed plane framework with finite deflections”, *Q. J. Mech. Appl. Math.* **17**:4 (1964), 451–469.
- [Williams et al. 2007] P. A. Williams, H. A. Kim, and R. Butler, “Bimodal buckling of optimised truss-lattice shear panels”, in *48th AIAA/ASME/ASCE/AHS/ASC structures, structural dynamics, and materials conference*, Honolulu, HI, 23–26 April 2007. paper no. AIAA-2007-2122.
- [Wittrick and Williams 1973] W. H. Wittrick and F. W. Williams, “Algorithm for computing critical buckling loads of elastic structures”, *J. Struct. Mech.* **1**:4 (1973), 497–518.
- [Yang et al. 2003] Y. B. Yang, J. D. Yau, and L. J. Leu, “Recent developments in geometrically nonlinear and postbuckling analysis of framed structures”, *Appl. Mech. Rev.* **56**:4 (2003), 431–449.

Received 20 Nov 2007. Revised 29 Feb 2008. Accepted 5 Mar 2008.

PHILIP A. WILLIAMS: P.Williams@bath.ac.uk

Department of Mechanical Engineering, University of Bath, Bath, BA2 7AY, United Kingdom

RICHARD BUTLER: R.Butler@bath.ac.uk

Department of Mechanical Engineering, University of Bath, Bath, BA2 7AY, United Kingdom

HYUNSUN A. KIM: H.A.Kim@bath.ac.uk

Department of Mechanical Engineering, University of Bath, Bath, BA2 7AY, United Kingdom

GILES W. HUNT: G.W.Hunt@bath.ac.uk

Department of Mechanical Engineering, University of Bath, Bath, BA2 7AY, United Kingdom

